Inorg. Chem. **2003**, *42*, 7995–8002

Solvent-Dependent Dynamics of the $MQ^{\bullet}\rightarrow Re^{II}$ Excited-State Electron Transfer in $[Re(MQ^{+})(CO)_3(dmb)]^{2+}$

Davina J. Liard,[†] Cornelis J. Kleverlaan,[‡] and Antonín Vlček, Jr.*[,†]

Department of Chemistry, Queen Mary and Westfield College, University of London, Mile End Road, London E1 4NS, United Kingdom, and Institute of Molecular Chemistry, Universiteit van Amsterdam, Nieuwe Achtergracht 166, NL-1018 WV Amsterdam, The Netherlands

Received June 9, 2003

The $Re\rightarrow MQ^{+}$ MLCT excited state of $[Re(MQ^{+})(CO)_3(dmb)]^{2+}$ (MQ^{+} = *N*-methyl-4,4′-bipyridinium, dmb = 4,4′-dimethyl-2,2′-bipyridine), which is populated upon 400-nm irradiation, was characterized by picosecond time-resolved IR and resonance Raman spectroscopy, which indicate large structural differences relative to the ground state. The $Re\rightarrow MQ^{+}$ MLCT excited state can be formulated as $[Re^{II}(MQ^{\bullet})(CO)_3(dmb)]^{2+}$. It decays to the ground state by a $MQ^{\bullet}\rightarrow Re^{II}$ back-electron transfer, whose time constant is moderately dependent on the molecular nature of the solvent, instead of its bulk parameters: formamides ∼ DMSO ∼ MeOH (1.2–2.2 ns) < THF, aliphatic nitriles (3.2–3.9 ns) << ethylene-glycol ∼ 2-ethoxyethanol (4.2–4.8 ns) < pyridine (5.7 ns) < $MeOCH_2CH_2OMe$ (6.9 ns) < PhCN (7.5 ns) < $MeNO_2$ (8.6 ns) <<< CH_2Cl_2, $ClCH_2CH_2Cl$ (25.9–28.9 ns). An approximate correlation was found between the back-reaction rate constant and the Gutmann donor number. Temperature dependence of the decay rate measured in CH_2Cl_2, MeOH, and BuCN indicates that the inverted $MQ^{\bullet}\rightarrow Re^{II}$ back-electron transfer populates a manifold of higher vibrational levels of the ground state. The solvent dependence of the electron transfer rate is explained by solvent effects on inner reorganization energy and on frequencies of electron-accepting vibrations, by interactions between the positively charged MQ^{+} pyridinium ring and solvent molecules in the electron-transfer product, that is the $[Re(MQ^{+})(CO)_3(dmb)]^{2+}$ ground state.

Introduction

The complex $[Re(MQ^{+})(CO)_3(dmb)]^{2+}$ (MQ^{+} = *N*-methyl-4,4′-bipyridinium, dmb = 4,4′-dimethyl-2,2′-bipyridine) undergoes a very interesting excited-state dynamics[1−6] following irradiation at 400 nm, which is summarized in Scheme 1 and by eqs 1−3. Optical excitation populates simultaneously $Re\rightarrow MQ^{+}$ and Re→dmb metal-to-ligand charge-transfer excited states, hereinafter called MLCT(MQ) and MLCT(dmb), respectively (eq 1). The ^{3}MLCT(dmb) excited state then undergoes a $dmb^{\bullet-}\rightarrow MQ^{+}$ interligand electron transfer, ILET (eq 2). The ^{3}MLCT(MQ) excited state, produced either by direct excitation or by ILET, decays to the ground state by the back electron-transfer reaction (eq 3).

$$[Re^{I}(MQ^{+})(CO)_3(dmb)]^{2+} \xrightarrow{h\nu} \underset{\text{MLCT(dmb)}}{[Re^{II}(MQ^{+})(CO)_3(dmb^{\bullet-})]^{2+}} + \underset{\text{MLCT(MQ)}}{[Re^{II}(MQ^{\bullet})(CO)_3(dmb)]^{2+}} \quad (1)$$

$$[Re^{II}(MQ^{+})(CO)_3(dmb^{\bullet-})]^{2+} \xrightarrow{\text{ILET}} [Re^{II}(MQ^{\bullet})(CO)_3(dmb)]^{2+} \quad (2)$$

$$[Re^{II}(MQ^{\bullet})(CO)_3(dmb)]^{2+} \xrightarrow{k_b} [Re^{I}(MQ^{+})(CO)_3(dmb)]^{2+} \quad (3)$$

The mechanism and dynamics of the ILET step were studied and understood only recently.[5,6] It is a (partly) adiabatic reaction that occurs from a vibrationally hot MLCT(dmb) excited state with time constants ranging from 8 to

* To whom correspondence should be addressed. E-mail: a.vlcek@qmul.ac.uk.
[†] University of London.
[‡] Universiteit van Amsterdam.

(1) Westmoreland, T. D.; Le Bozec, H.; Murray, R. W.; Meyer, T. J. *J. Am. Chem. Soc.* **1983**, *105*, 5952.
(2) Chen, P.; Curry, M.; Meyer, T. J. *Inorg. Chem.* **1989**, *28*, 2271.
(3) Chen, P.; Danielson, E.; Meyer, T. J. *J. Phys. Chem.* **1988**, *92*, 3708.
(4) Schoonover, J. R.; Chen, P.; Bates, W. D.; Dyer, R. B.; Meyer, T. J. *Inorg. Chem.* **1994**, *33*, 793.
(5) Liard, D. J.; Vlček, A., Jr. *Inorg. Chem.* **2000**, *39*, 485.
(6) Liard, D. J.; Busby, M.; Farrell, I. R.; Matousek, P.; Towrie, M.; Vlček, A., Jr. *J. Phys. Phem. A.*, in press.

10.1021/ic0346376 CCC: $25.00
Published on Web 11/07/2003

Scheme 1. Excited-State Behavior of $[Re(MQ^+)(CO)_3(dmb)]^{2+}$ [a]

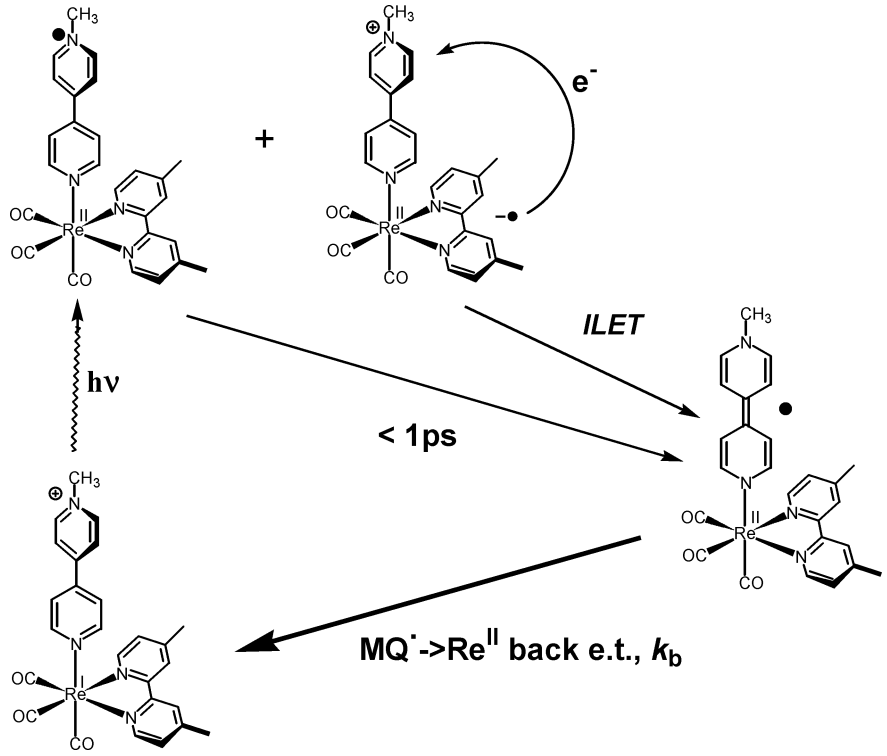

[a] The reacting MLCT(dmb) and product MLCT(MQ) states are actually spin-triplets. Spin labels and the intersystem crossing step are omitted for clarity.

18 ps, depending on the solvent. The mechanism of the back electron transfer (3) was not studied so far, although a time constant of 52 ns in 1,2-dichloroethane was mentioned in the literature.[3] It can be discussed from two different angles: either as a nonradiative decay of the MLCT(MQ) excited state or as a $MQ^{\bullet}\rightarrow Re^{II}$ back electron transfer.

Excited-state dynamics of $[Re^{I}(MQ^+)(CO)_3(dmb)]^{2+}$ provide an excellent case for understanding various aspects of electron transfer, such as the transition between adiabatic and nonadiabatic regimes, solvent and vibrational control, roles of outer- and inner-sphere reorganization, etc. ILET is a very efficient way to achieve an exceptionally fast photochemical charge separation. It is a rather common, albeit little studied, reaction that occurs in MLCT excited states of tris- and bis-polypyridine complexes[7−10] and which was also invoked[11] in the "DNA switch" $[Ru(bpy)_2(dppz)]^{2+}$. The $MQ^{\bullet}\rightarrow Re^{II}$ back electron transfer (3) is an energy-wasteful reaction. Understanding its mechanism and dynamics can further clarify relations between nonradiative decay of MLCT excited states and intramolecular electron transfer and can also suggest means of control of lifetimes of charge-separated states. The internal rotation of the $MQ^{\bullet}$ ligand from planar to twisted geometry during the $MQ^{\bullet}\rightarrow Re^{II}$ electron transfer (Scheme 1) and the high driving force makes this process related to other important excited-state electron-transfer reactions, for example in betaines,[12−15] acridinium dyes,[16,17] and donor−acceptor derivatives of biphenyl[18] or metal complexes containing a 4′-*p*-phenylterpyridine-triarylpyridinium ligand.[19−21] Similarly, intramolecular rotation can be coupled to optical charge-transfer excitation, as was observed, for example, in ruthenium(II) complexes containing a bpy ligand that bears a phenyl- or methylpyridinium group.[22,23]

Nonradiative excited-state decay in $[Re(L)(CO)_3(\alpha\text{-diimine})]^{n+}$ and analogous Ru(II) complexes is well understood for MLCT(diimine) excited states, where the electron is excited into the π^* orbital of the equatorial diimine ligand (diimine = derivatives of 2,2′-bipyridine, 1,10-phenanthroline or other polypyridines, 2-pyridyl-carbaldehyde-imine, and 1,4-diazabutadiene). Nonradiative decay rates are usually

(7) Shaw, G. B.; Brown, C. L.; Papanikolas, J. M. *J. Phys. Chem. A* **2002**, *106*, 1483.
(8) Waterland, M. R.; Kelley, D. F. *J. Phys. Chem. A* **2001**, *105*, 4019.
(9) Cushing, J. P.; Butoi, C.; Kelley, D. F. *J. Phys. Chem. A* **1997**, *101*, 7222.
(10) Pogge, J. L.; Kelley, D. F. *Chem. Phys. Lett.* **1995**, *238*, 16.
(11) Önfelt, B.; Lincoln, P.; Nordén, B.; Baskin, J. S.; Zewail, A. H. *Proc. Natl. Acad. Sci. U.S.A.* **2000**, *97*, 5708.
(12) Åkesson, E.; Johnson, A. E.; Levinger, N. E.; Walker, G. C.; DuBruil, T. P.; Barbara, P. F. *J. Chem. Phys.* **1992**, *96*, 7859.
(13) Kovalenko, S. A.; Eilers-König, N.; Senyushkina, T. A.; Ernsting, N. P. *J. Phys. Chem. A* **2001**, *105*, 4834.
(14) Åkesson, E.; Walker, G. C.; Barbara, P. F. *J. Chem. Phys.* **1991**, *95*, 4188.
(15) Lobaugh, J.; Rossky, P. J. *J. Phys. Chem. A* **1999**, *103*, 9432.
(16) Jones, G., II; Farahat, M. S.; Greenfield, S. R.; Gosztola, D. J.; Wasielewski, M. R. *Chem. Phys. Lett.* **1994**, *229*, 40.
(17) Horng, M. L.; Dahl, K.; Jones, G., II; Maroncelli, M. *Chem. Phys. Lett.* **1999**, *315*, 363.
(18) Maus, M.; Rettig, W.; Bonafoux, D.; Lapouyade, R. *J. Phys. Chem. A* **1999**, *103*, 3388.
(19) Lainé, P.; Amouyal, E. *Chem. Commun.* **1999**, 935.
(20) Lainé, P.; Bedioui, F.; Ochsenbein, P.; Marvaud, V.; Bonin, M.; Amouyal, E. *J. Am. Chem. Soc.* **2002**, *124*, 1364.
(21) Lainé, P.; Bedioui, F.; Amouyal, E.; Albin, V.; Berruyer-Penaud, F. *Chem. Eur. J.* **2002**, *8*, 3162.
(22) Damrauer, N. H.; McCusker, J. K. *J. Phys. Chem. A* **1999**, *103*, 8440.
(23) Shen, Y.; Walters, K. A.; Abboud, K.; Schanze, K. S. *Inorg. Chim. Acta* **2000**, *300*−*302*, 414.

interpreted[24−27] by using the energy-gap law. On the other hand, MLCT(L) states, where the electron is localized at the axial ligand, are rather rare, often difficult to populate by optical excitation. They can better be prepared by ILET, as in the case of $[Re(MQ^+)(CO)_3(dmb)]^{2+}$ studied herein, eq 2. Properties, dynamics, and lifetimes of MLCT(L) excited states are therefore much less understood than those of MLCT(diimine). Recently, Meyer et al. have studied[28] $[Re(L)(CO)_3(4,4'\text{-}R_2\text{-}bpy)]^+$ complexes where L represents various quinoidal electron-accepting ligands. Lifetime values of the MLCT(L) excited states cover a remarkably wide range, from 25 ns to 16 μs.[28]

Herein, we have concentrated on the MLCT(MQ) excited state of $[Re(MQ^+)(CO)_3(dmb)]^{2+}$. The rate of its nonradiative decay was investigated by time-resolved absorption spectroscopy in a wide range of solvents, while further information was obtained from the temperature dependence of the reaction rate. This study thus completes our understanding[5,6] of the dynamics of the excited states and electron-transfer reactions involved in the photochemistry of $[Re(MQ^+)(CO)_3(dmb)]^{2+}$. The principal conclusions of this work, namely that the medium can influence electron-transfer dynamics by affecting the intramolecular energy-accepting vibrations, have wider implications for the broad class of molecular processes in which electron transfer is accompanied by structural changes.

Experimental Section

$[Re(MQ^+)(CO)_3(dmb)](PF_6)_2$ was synthesized as described previously.[5,6] The solvents were obtained from Aldrich in spectroscopic quality (whenever available) and used without further purification, except for CH_2Cl_2, CH_3CN, BuCN, and THF which were dried by the standard techniques and distilled under N_2 atmosphere.

The reaction time constants measured in the course of this study occur in an experimentally difficult temporal range that is too fast for conventional nanosecond time-resolved spectrometers and too slow for ultrafast (femtosecond to picosecond) instruments. Herein, we have used a nanosecond spectrometer to obtain kinetic profiles of the probe light intensity at selected wavelengths within the transient absorption band, measured by a photomultiplier. The signal decay was analyzed by using a deconvolution procedure to separate the single-exponential absorbance decay from the instrument function. The latter was measured independently by the emission of rhodamine 6G. Deconvolution was carried out in Excel.

Nanosecond transient absorption was measured by irradiating the sample with 310 nm laser pulses of ca. 2 ns (fwhm) duration and 0.7 mJ energy (410 nm pulses were used in benzonitrile and nitromethane where the 310 nm light is absorbed by the solvent). These pulses were generated by an XPO-type parametric oscillator that was pumped by a Coherent Infinity Nd:YAG laser. The white probe light pulses were produced by a 450-W xenon lamp equipped with a Müller Electronik MSP05 pulsing unit, giving pulses of 0.5-ms duration, with a sampling rate of 1 Hz. Perpendicular orientation of the pump and probe beams was used. The probe beam then passed through an Oriel monochromator and the light intensity at 600 nm was detected by a P28 PMT (Hamamatsu), whose signal was recorded on a Tektronix TDS3052 (500 MHz) digital oscilloscope. The laser oscillator, Q-switch, lamp, shutter, and trigger were externally controlled with a homemade digital logic circuit, which allowed for synchronous timing. Temperature-dependent studies were performed with a cryostat. Samples were prepared with dry solvents, degassed with argon, and then cooled to −80 °C. This was then electrically heated in steps of 10 °C to room temperature. Time-resolved spectra were collected with use of the same experimental setup in which the detection system was replaced by an Acton Spectra-Pro spectrograph, gated CCD detector (Princeton Instruments ICCD-576EMG/RB), and OMA-4.[29]

Time-resolved IR, Kerr-gate resonance Raman and Kerr-gate emission used the equipment and procedures described in detail previously.[6,30−35] In short, the sample solution was excited (pumped) at 400 nm, using frequency-doubled pulses from a Ti:sapphire laser of ∼200-fs duration (fwhm) in the case of time-resolved visible and IR absorption spectroscopy, while pulses of 1−2-ps duration were used for Raman and emission studies. TRIR spectra were probed with IR (∼200 fs) pulses obtained by difference-frequency generation. The IR probe pulses cover a spectral range 150−200 cm^{-1} wide. Kerr-gate TR^3 spectra were measured with 1−2 ps, 400 nm pump pulses and probed at 600 or 400 nm, using an OPA or frequency-doubled Ti:sapphire laser pulses, respectively. Kerr gate was used to remove all long-lived emission from the Raman signal. TR^3 spectra were corrected for the Raman signal due to the solvent and the ground state by subtracting the spectra obtained at negative time delays (−50, −20 ps) and by subtracting any weak residual emission that passed through the Kerr gate. The sample solutions for picosecond TR^3 and TRIR experiments were flowed as 0.5 and 0.1 mm open jets, respectively.

Cyclic voltammograms were recorded on a Potentiostat Model 270/250 EG&G Instruments Inc., Princeton Applied Research. A home-built electrochemical cell was used with a three-electrode system: 0.5 mm^2 Pt working electrode, Pt-coil auxiliary electrode, and an Ag-coil pseudoreference electrode. All measurements were performed at a scan rate of 100 mV/s with 0.1 M Bu_4NPF_6 supporting electrolyte and 1−2 mM concentration of the complex. All redox potentials are reported against that of the ferrocene/ferrocenium (Fc/Fc^+) redox couple, which was used as an internal standard.

Stationary resonance Raman spectra were obtained from an acetonitrile solution, using a Dilor XY spectrometer with a 514.5-nm line of a Spectra Physics 2016 Ar^+ laser.

Results

Energetics of the MQ•→Re^II Electron Transfer. In principle, information on the driving force of the MQ•→Re^II

(24) Stufkens, D. J.; Vlček, A., Jr. *Coord. Chem. Rev.* **1998**, *177*, 127.
(25) Worl, L. A.; Duesing, R.; Chen, P.; Della Ciana, L.; Meyer, T. J. *J. Chem. Soc., Dalton Trans.* **1991**, 849.
(26) Caspar, J. V.; Meyer, T. J. *J. Phys. Chem.* **1983**, *87*, 952.
(27) Chen, P.; Meyer, T. J. *Chem. Rev.* **1998**, *98*, 1439.
(28) Claude, J. P.; Omberg, K. M.; Williams, D. S.; Meyer, T. J. *J. Phys. Chem. A* **2002**, *106*, 7795.
(29) Kleverlaan, C. J.; Stufkens, D. J.; Clark, I. P.; George, M. W.; Turner, J. J.; Martino, D. M.; van Willigen, H.; Vlček, A., Jr. *J. Am. Chem. Soc.* **1998**, *120*, 10871.
(30) Vlček, A., Jr.; Farrell, I. R.; Liard, D. J.; Matousek, P.; Towrie, M.; Parker, A. W.; Grills, D. C.; George, M. W. *J. Chem. Soc., Dalton Trans.* **2002**, 701.
(31) Matousek, P.; Parker, A. W.; Taday, P. F.; Toner, W. T.; Towrie, M. *Opt. Commun.* **1996**, *127*, 307.
(32) Towrie, M.; Parker, A. W.; Shaikh, W.; Matousek, P. *Meas. Sci. Technol.* **1998**, *9*, 816.
(33) Matousek, P.; Towrie, M.; Stanley, A.; Parker, A. W. *Appl. Spectrosc.* **1999**, *53*, 1485.
(34) Matousek, P.; Towrie, M.; Ma, C.; Kwok, W. M.; Phillips, D.; Toner, W. T.; Parker, A. W. *J. Raman Spectrosc.* **2001**, *53*, 1485.
(35) Towrie, M.; Grills, D. C.; Matousek, P.; Parker, A. W.; George, M. W. *Appl. Spectrosc.* **2003**, *57*, 367.

Table 1. Time and Rate Constants of the $MQ^{\bullet}\rightarrow Re^{II}$ Back Reaction, Selected Solvent Properties, and the Estimated Driving Force

entry	solvent	τ_b, ns	k_b, $10^8 s^{-1}$	ϵ_s[a]	$1/\epsilon_{op} - 1/\epsilon_s$	donor no.[b]	$\langle\tau_s\rangle$,[c] ps
1	*N*-methylformamide	1.24	8.06	182.4	0.485	49.0	5.7
2	DMF	1.25	8.00	36.7	0.463	26.6	0.92
3	DMSO	1.48	6.76	46.7	0.437	29.8	1.79
4	MeOH	2.11	4.74	32.7	0.538	18.0	0.94
5	CD_3OD	2.21	4.52				
6	formamide	2.18	4.59	111.0	0.469	36.0	5
7	THF	3.23	3.10	7.6	0.376	20.0	5
8	CH_3CH_2CN	3.47	2.88	27.2	0.501	16.1	1.15
9	CH_3CN	3.56	2.81	37.5	0.529	14.1	0.26
10	$CH_3(CH_2)_2CN$	3.71	2.70	20.3	0.474	16.6	1.85
11	$(CH_3)_2CHCN$	3.82	2.62	20.4	0.483	15.4	3.6
12	$CH_3(CH_2)_3CN$	3.88	2.58	19.7	0.462		1.88
13	$HOCH_2CH_2OH$	4.23	2.36	37.7	0.461	20.0	10.6
14	$EtOCH_2CH_2OH$	4.84	2.07	29.6	0.471		
15	pyridine	5.65	1.77	12.4	0.360	33.1	
16	$MeOCH_2CH_2OMe$	6.88	1.45	7.2	0.586		
17	PhCN	7.48	1.34	25.2	0.390	11.9	5.1
18	CH_3NO_2	8.56	1.17	35.9	0.498	2.7	0.41
19	CH_2Cl_2	25.89	0.39	8.9	0.383	0.0	0.56
20	$ClCH_2CH_2Cl$	28.89	0.35	10.4	0.384	0.0	

[a] Reference 42. [b] References 15 and 41. [c] References 17 and 43−46. ϵ_{op} = optical dielectric constant.[42]

electron transfer (3) could be obtained from spectral fitting of the emission band due to radiative decay of the ^{3}MLCT(MQ) state, which yields the emission energy and reorganization energy.[36] This band was indeed observed in stationary emission spectra[1,3] of $[Re(MQ^+)(CO)_3(bpy)]^{2+}$ and picosecond time-resolved Kerr-gate emission spectra[6] of $[Re(MQ^+)(CO)_3(dmb)]^{2+}$. However, its very low intensity, broadness, and overlap with the residual ^{3}MLCT(dmb) emission prevents such fitting. Alternatively, the driving force can be estimated as a difference of the energy of the ^{3}MLCT(dmb) excited state and the ILET driving force, which was determined[6] electrochemically. On the basis of very similar[6] IR and emission spectra of the ^{3}MLCT(dmb) state in $[Re(MQ^+)(CO)_3(dmb)]^{2+}$ and in the model complex $[Re(Etpy)(CO)_3(dmb)]^+$, we can also assume that the respective excited-state structures and energies are very similar. Values of 2.70, 2.57, and 2.78 eV were determined for the MLCT(dmb) excited-state free energy of $[Re(Etpy)(CO)_3(dmb)]^+$ in fluid CH_3CN, $ClCH_2CH_2Cl$, and a poly(methyl methacrylate) polymer film, respectively,[28,37,38] indicating only very limited medium dependence. By using these values and the ILET driving force, we can estimate the driving force of reaction 3 as 2.24 and 2.11 eV in CH_3CN and $ClCH_2CH_2Cl$, respectively. The latter value can be used also for CH_2Cl_2. Generally, it appears that the driving force of the $MQ^{\bullet}\rightarrow Re^{II}$ electron transfer is only little dependent on the medium. This assumption is supported by the fact that the emission from the ^{3}MLCT(MQ) state of $[Re(MQ^+)(CO)_3(bpy)]^{2+}$ occurs at very similar energies in CH_3CN and $ClCH_2CH_2Cl$, 1.88 and 1.78 eV, respectively,[6,39] and by very similar values of the difference between the potentials of the reversible $MQ^+/MQ^{\bullet}$ reduction and the quasireversible Re^I/Re^{II} oxidation in CH_3CN, CH_2Cl_2, and THF: 2.46, 2.39, and 2.57 V, respectively. In conclusion, we assume that the driving force of the back reaction in all the solvents investigated lies within the range 2.1−2.3 eV. The values used herein are close to the 2.31 eV driving force of the $BIQD^{\bullet-}\rightarrow Re^{II}$ back reaction in the MLCT(BIQD) excited state of $[Re(BIQD)(CO)_3(dmb)]^+$ (BIQD = benz[*g*]isoquinoline-5,10-dione), whose emission band peaks at 688 nm.[28]

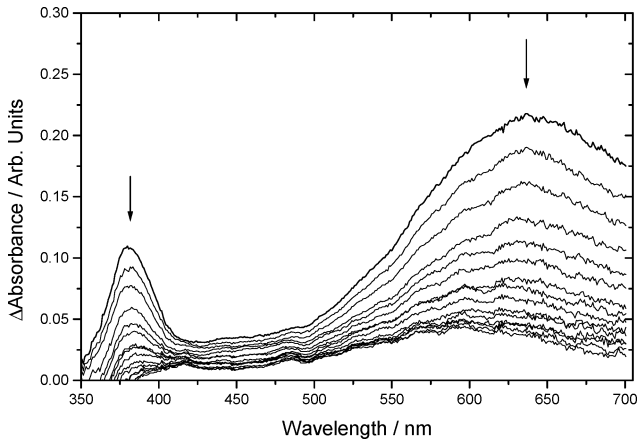

Figure 1. Nanosecond time-resolved absorption spectra of $[Re(MQ^+)(CO)_3(dmb)]^{2+}$ in CH_2Cl_2. The spectral evolution is indicated by the arrows. The first spectrum was measured coincidently with 310-nm excitation. Time difference between the spectra is 5 ns. (τ_b values were determined from continuous kinetic traces at 600 nm, recorded by a fast PMT, see Experimental Section.)

Importantly, all the energetic considerations show that the driving force values are much larger than any realistic estimate of the reorganization energy λ. It can thus be concluded that the $MQ^{\bullet}\rightarrow Re^{II}$ electron transfer occurs deep in the Marcus inverted region.

Solvent-Dependent Kinetics of the $MQ^{\bullet}\rightarrow Re^{II}$ Electron Transfer. Decay times τ_b of the ^{3}MLCT(MQ) excited state were measured from the deacy of the intense $MQ^{\bullet}$ transient absorption bands, Figure 1. The values are summarized in Table 1, together with the corresponding rate constants, k_b

(36) Omberg, K. M.; Chen, P.; Meyer, T. J. In *Electron Transfer−From Isolated Molecules to Biomolecules*; Part II, Advances in Chemical Physics. Vol. 106; Jortner, J., Bixon, M., Eds.; J. Wiley & Sons: New York, 1999; p 553.
(37) Dattelbaum, D. M.; Omberg, K. M.; Schoonover, J. R.; Martin, R. L.; Meyer, T. J. *Inorg. Chem.* **2002**, *41*, 6071.
(38) Dattelbaum, D. M.; Meyer, T. J. *J. Phys. Chem. A* **2002**, *106*, 4519.
(39) Mecklenburg, S. L.; Opperman, K. A.; Chen, P.; Meyer, T. J. *J. Phys. Chem.* **1996**, *100*, 15145.

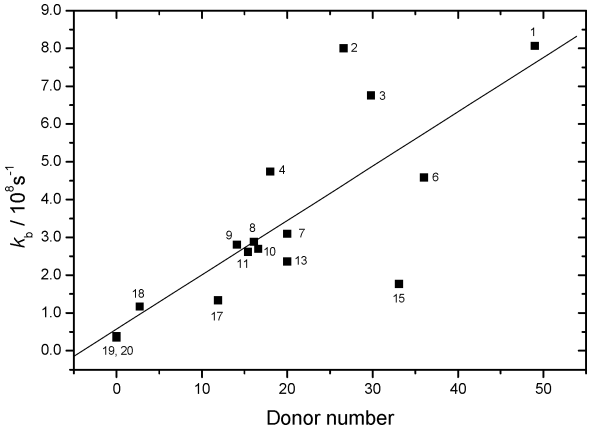

Figure 2. Correlation between the rate constant k_b of the back electron transfer (3) and the solvent donor number. The numbers correspond to the entries in Table 1. The k_b values were determined with an accuracy of about ±5%.

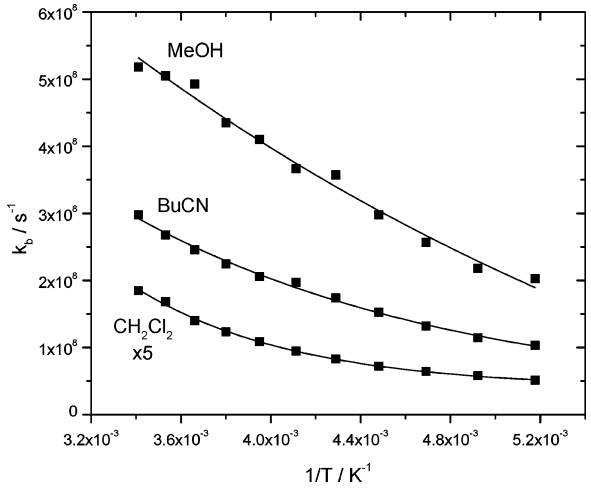

Figure 3. Temperature dependence of the rate constant k_b of the back electron transfer (eq 3) in MeOH, BuCN, and CH_2Cl_2. Fits according to eq 4.

($k_b = 1/\tau_b$), and the relevant solvent properties. The ^{3}MLCT-(MQ) decay times and back-reaction rate constants do not correlate with any of the usual solvent parameters such as the dielectric constant ϵ_s, solvent function ($1/\epsilon_{op} - 1/\epsilon_s$), or the solvent relaxation time. Moreover, the solvent dependence of the MQ•→Re^{II} rate constant cannot be accounted for by driving force variations. This would, for example, require a sharp increase of driving force on going from CH_3CN to chlorinated solvents $ClCH_2CH_2Cl$ or CH_2Cl_2, which was not observed. On the contrary, the driving force estimated for CH_3CN is slightly higher than that for CH_2Cl_2, vide supra. (Note that driving force estimates are most reliable in these two solvents.) Nevertheless, the MQ•→Re^{II} dynamics show an interesting dependence on the chemical nature of the solvent. The time constants increase in the following order: formamides ∼ DMSO ∼ MeOH (1.2−2.2 ns) < THF, aliphatic nitriles (3.2−3.9 ns) << ethyleneglycol ∼ 2-ethoxyethanol (4.2−4.8 ns) < pyridine (5.7 ns) < $MeOCH_2CH_2OMe$ (6.9 ns) < PhCN (7.5 ns) < $MeNO_2$ (8.6 ns) <<< CH_2Cl_2, $ClCH_2CH_2Cl$ (25.9−28.9 ns). A reasonable correlation was found between the back-reaction rate constant and the Gutmann donor number,[40,41] D_N, see Figure 2.

The temperature dependence of the back-reaction rate constant was investigated in CH_2Cl_2, BuCN, and MeOH, see Figure 3. Experimental rate constants can be fitted to an Arrhenius-type equation

$$k_b = a_0 + a_1 \exp(-E_a/RT) \qquad (4)$$

that is often used to analyze excited-state decay of polypyridine complexes.[24] The apparent activation energy E_a determined in CH_2Cl_2 is rather low: 980 cm^{-1}. Its value decreases in BuCN and MeOH to 470 and 200−380 cm^{-1}, respectively. However, the fits are less accurate than in CH_2Cl_2. The data in MeOH actually indicate a systematic deviation from the Arrhenius-type behavior. The constant term a_0 is substantial, ca. 7.9 × 10^6 s^{-1} in CH_2Cl_2. This behavior indicates the presence of two reaction pathways, one of which involves barrier crossing, while the other is temperature independent, occurring via a weak coupling between the MLCT(MQ) excited state and the ground state. About 20% of the back reaction follows the temperature-independent channel. The temperature dependence of the rate constant was also fitted to eq 5, which describes nonadiabatic electron transfer in the Marcus inverted region.[47]

$$k_b = \frac{V_{el}^2}{\hbar(4\pi\lambda_o k_B T)^{1/2}} e^{-S} \sum_{m=0} \frac{S^m}{m!} \times \exp\left[-\frac{(\Delta G^o + \lambda_o + m h\nu_i)^2}{4\lambda_o k_B T}\right] \qquad (5)$$

This approach assumes an existence of many reaction channels, each of which populates a different vibrational level m of the ground-state $[Re(MQ^+)(CO)_3(dmb)]^{2+}$, Figure 4. In other words, electron transfer activates high-frequency vibrations which accept the excess of free energy released during the reaction.[36,47−49] Population of higher vibrational levels of the product effectively decreases the driving force, thus accelerating the inverted reaction, see Figure 4. These high-frequency vibrations are characterized by a single average energy $h\nu_i$. All other low-frequency intramolecular and solvent modes are treated classically and included in the outer reorganization energy λ_o. The dimensionless parameter S describes the average relative structural difference between the ground and excited state. $-\Delta G°$ is the

(40) Gritzner, G. *J. Mol. Liq.* **1997**, *73*, *74*, 487.
(41) Linert, W.; Gutmann, V. *Coord. Chem. Rev.* **1992**, *117*, 159.
(42) Riddick, J. A.; Bunger, W. B.; Sakano, T. K. *Organic Solvents*; Wiley: New York, 1986.
(43) Kahlow, M. A.; Kang, T. J.; Barbara, P. F. *J. Chem. Phys.* **1988**, *88*, 2372.
(44) Jarzeba, W.; Walker, G. C.; Johnson, A. E.; Barbara, P. F. *Chem. Phys.* **1991**, *152*, 57.
(45) Horng, M. L.; Gardecki, J. A.; Papazyan, A.; Maroncelli, M. *J. Phys. Chem.* **1995**, *99*, 17311.
(46) Shirota, H.; Pal, H.; Tominaga, K.; Yoshihara, K. *J. Phys. Chem.* **1996**, *100*, 14575.
(47) Brunschwig, B. S.; Sutin, N. *Comments Inorg. Chem.* **1987**, *6*, 209.
(48) Jortner, J.; Bixon, M. *J. Chem. Phys.* **1988**, *88*, 167.
(49) Bixon, M.; Jortner, J. In *Electron Transfer−From Isolated Molecules to Biomolecules*; Part I, Advances in Chemical Physics. Vol. 106; Jortner, J., Bixon, M., Eds.; J. Wiley and Sons, Inc.: New York, 1999; p 35.

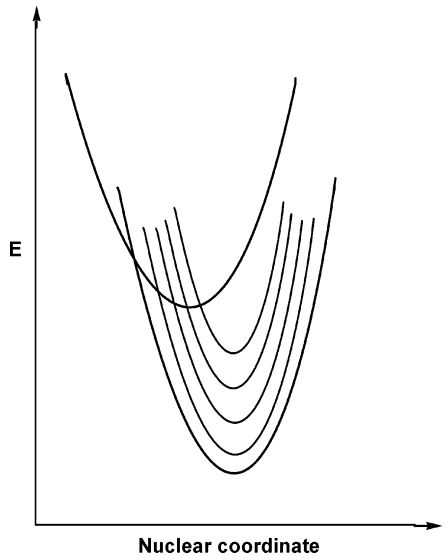

Figure 4. Potential energy curves describing inverted electron transfer.

electron-transfer driving force and V_{el} is the electronic coupling. In this approach, the reaction channels which involve very low vibrational quanta m account for the temperature dependence of the reaction rate while those at higher m values account for the temperature-independent contribution to the reaction rate, Figure 4. (Note that the relative importance of the reaction channels rapidly diminishes for high m values because of the $m!$ term in eq 5.)

Acceptable fits were obtained in CH_2Cl_2 for several combinations of parameters V_{el}, λ_o, and $h\nu_i$. (The values of $\Delta G°$ and S were kept constant at -2.11 eV and 1.4, respectively.[50] A possible small temperature dependence[51] of λ_o was neglected.) By comparing the results, we can conclude that the electronic coupling V_{el} is at least 30 cm^{-1} but not higher than 500 cm^{-1}. (Note that the value of 153 cm^{-1} that was found[28] for $BIQD^{\bullet-}\rightarrow Re^{II}$ in $[Re(BIQD)(CO)_3(dmb)]^+$ would fall into this range.) The fits predict λ_o to lie in the range 4310−5410 cm^{-1} while $h\nu_i$ ranges from 950 to ca. 970 cm^{-1}. For comparison, $\lambda_o = 3660$ cm^{-1} and $h\nu_i = 1625$ cm^{-1} were determined for the $BIQD^{\bullet-}\rightarrow Re^{II}$ back electron transfer in $ClCH_2CH_2Cl$ by emission fitting.[28] The data obtained in BuCN are less accurate than those from CH_2Cl_2. Nevertheless, the fits to eq 5 show that both λ_o and $h\nu_i$ are higher in BuCN: 5500−8000 and ∼1100 cm^{-1}, respectively. The data measured in MeOH give rather poor fits which, nevertheless, indicate still slightly higher values of λ_o and $h\nu_i$ than in BuCN.

Discussion

Previous spectroscopic studies[4,6] have established that the ^{3}MLCT(MQ) excited state of $[Re(MQ^+)(CO)_3(dmb)]^{2+}$ can be formulated as $[Re^{II}(MQ^{\bullet})(CO)_3(dmb)]^{2+}$. The time-resolved resonance Raman spectrum (Figure 5) of the

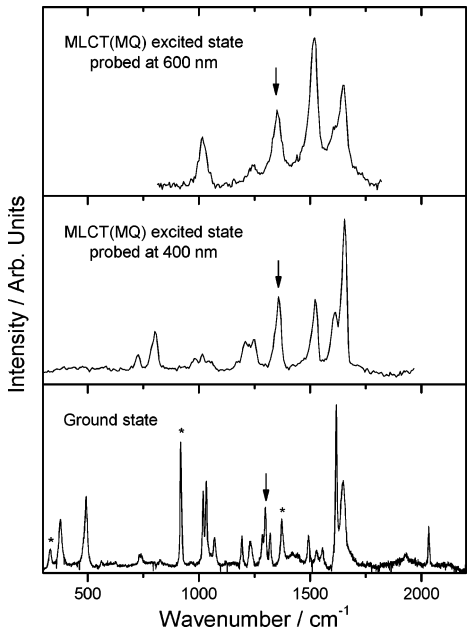

Figure 5. Comparison of resonance Raman spectra of the ground state and MLCT(MQ) excited state of $[Re(MQ^+)(CO)_3(dmb)]^{2+}$ in CH_3CN. Top: MLCT(MQ) excited-state spectrum measured by ps Kerr-gate TR[3] at 500 ps after excitation with a probe wavelength of 600 nm. Middle: MLCT(MQ) excited-state spectrum measured by ps Kerr-gate TR[3] at 100 ps after excitation with a probe wavelength of 400 nm. The Raman bands occur at 1651, 1608 (sh), 1518, 1354, ∼1247, 1018, 801, and 725 cm^{-1}. The 1354-cm^{-1} peak (marked ↓), that is due to a MQ $\nu(CC)_{interring}/\delta(CCH)/\nu(CC)$ vibration, experiences the largest shift (+55 cm^{-1}) from its position in the ground-state spectrum. See ref 6 for the assignment. Bottom: Ground-state preresonance Raman spectrum, probed at 514.5 nm. See ref 6 for the assignment. An asterisk indicates solvent bands.

^{3}MLCT(MQ) excited state of $[Re(MQ^+)(CO)_3(dmb)]^{2+}$ clearly shows that the MQ ligand has very different structures in the ^{3}MLCT(MQ) excited state and the ground state: planar quinoidal and twisted,[52] respectively. These structural differences concern namely the dihedral angle between the two rings and the inter-ring C−C bond, see Scheme 1. In addition, large structural changes upon $Re\rightarrow MQ^+$ excitation are demonstrated by the preresonance Raman spectrum of $[Re(MQ^+)(CO)_3(dmb)]^{2+}$ (Figure 5), which shows strongly enhanced bands due to the vibrations of the MQ^+ and dmb ligands as well as of the A′(1) in-phase ν(CO) vibration of the $Re(CO)_3$ moiety. At the same time, the picosecond time-resolved IR spectrum of the ^{3}MLCT(MQ) excited state (Figure 6) shows that all the ν(CO) vibrations occur at much lower wavenumbers in the ground state than in the ^{3}MLCT(MQ) excited state, -76 cm^{-1} on the average, indicating a considerable increase of electron density on the $Re(CO)_3$ moiety upon the $MQ^{\bullet}\rightarrow Re^{II}$ electron transfer. This is connected with lengthening of the C≡O bonds. Moreover, the bond angles also change, as is demonstrated by the change of the whole ν(CO) spectral pattern, whereby the lower band due to in-plane A″ and out-of-phase A′(2) vibrations are split into two bands whose wavenumbers are quite far apart in the ^{3}MLCT(dmb) state but merged in the ground state (see Figure 6).

(50) Fitting with a lower estimate of $S = 0.7$ gives values of $h\nu_i$ between 1200 and 1300 cm^{-1} but rather high λ_o. It appears that the highest possible limit for $h\nu_i$ is 1230 cm^{-1}. A combination of values $h\nu_i >$ 970 cm^{-1} and $S = 1.4$ never afforded an acceptable fit. In BuCN, the highest possible limit for $\hbar\nu_i$ is ∼1380 cm^{-1}.

(51) Derr, D. L.; Elliott, C. M. *J. Phys. Chem. A* **1999**, *103*, 7888.

(52) Busby, M.; Liard, D. J.; Motevalli, M.; Toms, H.; Vlček, A., Jr. *Inorg. Chim. Acta*. **2003**, in press.

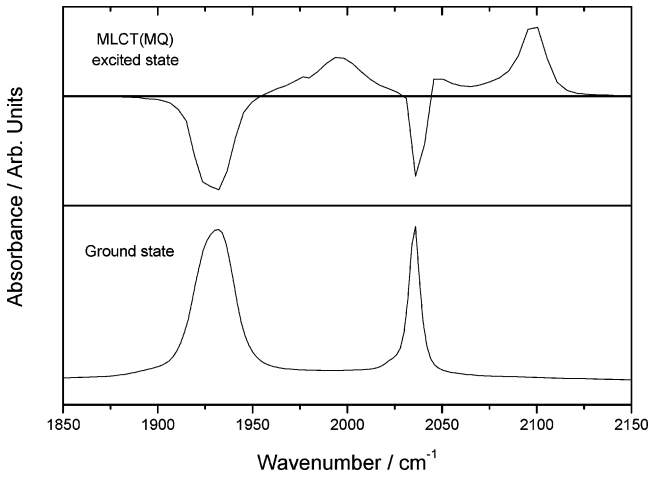

Figure 6. Comparison of IR spectra of the ground state and MLCT(MQ) excited state of $[Re(MQ^+)(CO)_3(dmb)]^{2+}$ in CH_3CN. Top: MLCT(MQ) excited-state spectrum measured by TRIR at 100 ps after excitation. A difference between the spectra measured with and without excitation is shown. Negative peaks correspond to the depleted ground-state population. Positive peaks belong to the MLCT(MQ) state. They occur at 2096, ~2040, and 1993 cm^{-1} corresponding to A′(1), A′(2), and A″ ν(CO) vibrations, respectively. The ~2040-cm^{-1} peak overlaps with the negative ground-state band. Bottom: Ground-state FTIR spectrum with 2036 and 1931 cm^{-1} bands corresponding to A′(1) and A′(2) + A″ ν(CO) vibrations, respectively.

The ^{3}MLCT(MQ) excited state decays nonradiatively to the ground state by a MQ•→Re^{II} electron transfer on a time scale of 1−30 ns, see Table 1. The rate constant depends on the solvent, but the temperature dependence is weak. The MQ•→Re^{II} electron transfer occurs with a large driving force (≥2.1 eV), deeply in the Marcus inverted region. Analysis of the temperature dependence of the reaction rate reveals that the MQ•→Re^{II} back electron transfer involves both thermally activated barrier crossing and a barrierless tunneling that populates higher vibrational levels of the ground state. The time constant of the MQ•→Re^{II} electron transfer in $ClCH_2CH_2Cl$ is comparable to that of BIQD•→Re^{II} in the MLCT(BIQD) excited state of the analogous complex $[Re(BIQD)(CO)_3(dmb)]^+$, for which a value of 25−32 ns was determined in CH_2ClCH_2Cl.[28] The MQ•→Re^{II} electron transfer occurs with a comparable or slightly higher electronic coupling, higher outer reorganization energy, and lower wavenumber of the accepting vibrational mode, vide supra. The larger outer reorganization energy can be caused by stronger solvation changes due to the creation of a positive charge upon the MQ•→Re^{II} electron transfer, which is rather localized on the MQ^+ pyridinium ring. The smaller size of MQ^+ as compared with BIQD may also contribute. The lower wavenumber of the accepting mode can be explained by a large contribution from the twisting vibration around the MQ inter-ring C−C bond, for which a rather low wavenumber of ca. 240 cm^{-1} is expected based on vibrational analysis of biphenyls.[53]

The rate of the MQ•→Re^{II} back electron transfer depends on the chemical nature of the solvent molecules, instead of bulk solvent parameters. The reaction is the fastest in good electron donors, which are known to strongly solvate cations, slower in weakly solvating $MeNO_2$, and slowest in chlorinated solvents. This conclusion is supported by the observed correlation between the rate constant and the donor number, Figure 2. However, this effect cannot be explained by a thermodynamic stabilization of the ground state by solvation, for which there is no electrochemical evidence.[6] Moreover, this would increase the driving force and, hence, slow the reaction down in donor solvents, contrary to the experimental observation.

In fact, acceleration of the MQ•→Re^{II} electron transfer in strongly donating solvents shows that the stronger solvation of the electron-transfer product, that is the $[Re^I(MQ^+)(CO)_3(dmb)]^{2+}$ ground state, increases the outer reorganization energy and the average frequency of the accepting vibration. (Note that an increase of λ_o and/or $h\nu_i$ decreases the activation energy in the Marcus inverted region, where $-\Delta G^\circ > \lambda_o$, see eq 5.) This conclusion is fully supported by the observed sharp drop of the apparent Arrhenius activation energy on going from CH_2Cl_2 to BuCN and MeOH and, especially, by analyzing the temperature-dependent rates according to eq 5, vide supra. It has to be stressed that the increase of λ_o with the solvent donor strength reflects changes in *molecular* properties of the solvent. It is not related to the usual bulk electrostatic properties which are characterized by the "solvent function" $1/\epsilon_{op} - 1/\epsilon_s$. (No correlation between k_b and the solvent function exists.) The stronger solvation of the cationic MQ^+ ligand in the electron-transfer product $[Re^I(MQ^+)(CO)_3(dmb)]^{2+}$ in donating solvents will increase structural differences between the MLCT(MQ) state, where MQ• is formally neutral, and the ground state, where MQ^+ is a cation with a rather localized positive charge. Better solvation results in larger charge separation in the ground state which, in turn, affects the bonding within the MQ^+ ligand and, hence, the average frequency of the accepting vibrational mode. This type of behavior seems to be more general. For example, solvent effects on the inner reorganization energy and high-frequency vibrational modes were found also for highly inverted back electron transfer in betaines.[13,54] The conclusion that molecular solvent properties affect the dynamics of inverted electron transfer through the inner reorganization energy and quantized vibration modes could have important implications for developing new means of control of electron-transfer processes, for example by supramolecular complexation.

Finally, an interesting question arises, whether the back reaction (3) should better be viewed as an inverted MQ•→Re^{II} electron transfer or as a nonradiative decay of a MLCT(MQ) excited state. This question is, to some extent, formal since both these limiting views are conceptually similar and described by the same formalism, that is the Landau−Zener electron tunneling probability multiplied by the Franck−Condon weighted density of states, which determines the probability that the system attains the transition state geometry. In the limiting case of a nonradiative decay, the potential energy curves of the excited and ground state are not supposed to cross and the decay occurs solely by

(53) Michelsen, H.; Kleboe, P.; Hagen, G.; Stroyer-Hansen, T. *Acta Chem. Scand.* **1972**, *26*, 1576.

(54) Zong, Y.; McHale, J. L. *J. Chem. Phys.* **1997**, *106*, 4963.

tunneling into high vibrational levels of the ground state, described by the well-known energy-gap law. Any temperature dependence of the decay rate, if observed at all, is usually attributed to a thermal population of high-lying, fast-decaying excited states. On the other hand, the limiting inverted electron-transfer mechanism assumes a multitude of reaction channels populating different vibrational levels of the ground state, Figure 4. Each of these channels is characterized by a different activation energy, some of them being (nearly) activationless. Herein, it was found that the temperature-dependent rate constants follow the electron-transfer-type behavior, as described by eq 5, indicating that the $MQ^{\bullet} \rightarrow Re^{II}$ process should better be viewed as a nonadiabatic inverted electron transfer than a nonradiative excited-state decay. It is remarkably fast, being accelerated by large contribution from quantal intramolecular energy-accepting vibrational modes of the ground-state product, that are made available by the large accompanying structural reorganization and charge redistribution. This case underlines the close conceptual link between an intramolecular electron transfer and a nonradiative decay of a charge-transfer excited state.

Acknowledgment. P. Matousek and M. Towrie (CLRC, Rutherford Appleton Laboratory) are thanked for their help with the measurements of the picosecond time-resolved IR and resonance Raman spectra while Frank Vergeer (Universiteit van Amsterdam) is acknowledged for his help with nanosecond measurements. Funding from EPSRC and the COST Action D14 is gratefully acknowledged.

IC0346376